

# Sour Top-of-the-Line Corrosion in the Presence of Acetic Acid

M. Singer,<sup>‡</sup>\* A. Camacho,<sup>\*\*</sup> B. Brown,<sup>\*</sup> and S. Nešić<sup>\*</sup>

## ABSTRACT

*Under stratified flow and dewing conditions, internal corrosion can occur at the top of horizontal pipelines where continuous injection of corrosion inhibitors does not have a mitigating effect. This research work presents an experimental study of the influence of the presence of hydrogen sulfide (H<sub>2</sub>S; up to 0.13 bars) and acetic acid (HAc; up to 1,000 ppm) on carbon dioxide (CO<sub>2</sub>) top-of-the-line corrosion. The study was performed in a 10 cm (4 in) internal diameter flow loop with system conditions constant at 70°C, 2 bars partial pressure CO<sub>2</sub>, 3 bars total pressure, 5 m/s gas velocity, and a water condensation rate of 0.25 mL/m<sup>2</sup>/s. A comprehensive analysis on the effect of these parameters (partial pressure of H<sub>2</sub>S and concentration of acetic acid) on the type of corrosion product film formed at the top of the line is performed.*

**KEY WORDS:** acetic acid, carbon dioxide, hydrogen sulfide, top-of-the-line corrosion

## INTRODUCTION

Top-of-the-line corrosion (TLC) was first identified in the 1960s<sup>1</sup> and has become a growing concern for the oil and gas industry over the past two decades. Many field cases have been published from both onshore and offshore environments.<sup>2-7</sup> This type of corrosion occurs in stratified flow when significant temperature gradients exist between the outside environment

and the process fluid, therefore leading to water condensation on the internal walls of the pipe line. The presence of this condensed water can induce severe general and pitting corrosion problems, typically on the upper part of the pipe (between 9 o'clock and 3 o'clock). Mitigation methods for TLC corrosion are limited and ineffective in some cases, so research toward understanding the mechanisms of corrosion are necessary.

Two main sub-categories of TLC can be identified depending on whether the corrosion mechanism is carbon dioxide (CO<sub>2</sub>)- or hydrogen sulfide (H<sub>2</sub>S)-dominated. To be fair, the boundaries delimiting what is a sweet or a sour corrosion are not even clear today, but are most likely linked to the type of corrosion product film forming at the metal surface.

TLC in sweet conditions has been the focus of intensive research over the past fifteen years and the main corrosion mechanisms involved are now identified, although not well understood. The severity of TLC in sweet conditions depends mostly on the condensation rate, the gas temperature, the gas flow rate, the CO<sub>2</sub> partial pressure, and the presence of organic acid.<sup>8</sup> Pipe inspections often reveal corrosion over extended areas of the top of the pipeline associated with breakdowns of an otherwise protective FeCO<sub>3</sub> layer. Field experience in this domain is also growing and a lot of research work has already been published.<sup>9-13</sup>

In sour conditions, the mechanisms governing TLC seem largely different than those observed in sweet conditions. Several pipe failures have been attributed to sour TLC,<sup>1,5-7</sup> although the real control-

Submitted for publication July 20, 2010; in revised form, January 31, 2011.

<sup>‡</sup> Corresponding author. E-mail: singer@ohio.edu.

<sup>\*</sup> Institute for Corrosion and Multiphase Technology, Ohio University, 342 West State St., Athens, OH 45701.

<sup>\*\*</sup> Lloyd's Register Capstone, Houston, TX.

ling parameters were often unclear. Limited research work has been published on sour TLC,<sup>14-16</sup> and these often lead more to interrogation than real answers. Although no firm conclusion can be made at this stage, some important characteristics of sour TLC have been proposed:<sup>17</sup>

- Sour TLC does not seem to be as serious or as common as sweet TLC.
- The condensation rate may not be the main controlling parameter as it is in sweet TLC.
- The severity of the attack seems to depend on the type and protectiveness of the iron sulfide film formed at the condensed water/steel interface.
- Gas temperature, consequently, could be a key factor because it directly affects the phase identity and characteristics of the formed iron sulfide.

The influence of parameters such as temperature, H<sub>2</sub>S partial pressure, concentration of acetic acid (HAc), or exposure time on the characteristics of the iron sulfide (FeS) scale formed at the top of the line is the focus of ongoing research. Much more experimental work has been performed on sour bottom-of-the-line corrosion, especially looking at the effect of small amounts of H<sub>2</sub>S.<sup>18-21</sup> The subsequent reduction of the corrosion rate as compared to a baseline pure CO<sub>2</sub> environment is associated with the formation of a protective mackinawite film. The presence of organic acids, so aggressive in TLC in a sweet environment,<sup>9</sup> has been reported to affect greatly the protectiveness of mackinawite and lead to localized corrosion at the bottom of the line.<sup>22</sup> There is no reason to believe that the organic acids, condensing together with the water at the top of the line, will not play a key role in the severity of sour TLC. However, different environmental conditions can lead to the formation of various thermodynamically stable types of FeS<sup>23</sup> and, consequently, various corrosion scenarios. However, the links between the types of FeS formed and their specific corrosion protectiveness have not yet been established. It is important to mention that even the definition of what constitutes a sour environment (as opposed to sweet environment) is subject to debate. The sweet/sour corrosion regime proposed by Pots, et al.,<sup>24</sup> is still widely used in the industry, though its domain of validity is very narrow. Recent analysis performed on the basis of this ratio highlighted the uncertainty surrounding the thermodynamic data and concluded to its relative unsuitability as an industry guideline.<sup>25</sup>

The objective of this paper was to provide experimental results obtained through a parametric study of the effect of the partial pressures of H<sub>2</sub>S and CO<sub>2</sub> as well as the presence of acetic acid on the top-

of-the-line corrosion rate. The results presented in this paper were obtained through experiments that focused on top-of-the-line and bottom-of-the-line corrosion. In this article, only the top-of-the-line results are taken into account. The bottom-of-the-line corrosion results are already published in previous NACE conference proceedings.<sup>8,14,22</sup> References are made to these papers in the following sections and the reader is advised to refer to these previous publications for more details on the experimental procedure and conditions.

## EXPERIMENTAL PROCEDURES

The following sections related to the experimental procedure focusing on bottom-of-the-line corrosion<sup>22</sup> have already been reported in NACE CORROSION/2007 and CORROSION/2009 with the sections focusing on CO<sub>2</sub> top-of-the-line corrosion.<sup>8</sup> Consequently, the basic description of the equipment and the procedure has been derived from these two previously published works. Some clarifications have been added to reflect the focus of this paper.

### Experimental Loop

Three, different, large-scale flow loops were used in this study. The flow loops, made of Type 316 (UNS S31600)<sup>(1)</sup> stainless steel and Alloy C276 ([UNS N10276] for the H<sub>2</sub>S experiments), all have very similar characteristics that can be divided into three main parts: the tank, the pump, and the loop.

- The tank is used for liquid phase conditioning and heating. Filled with 300 gallons of deionized water, a set of immersion heaters controls the temperature of the fluid in the tank, which, in turn, controls the vapor phase temperature. Acetic acid is added to the deionized water in the tank, as needed, to reach the concentration requirements of the tests.
- A positive displacement progressive cavity pump or gas blower is used to move the liquid or the gas phase.
- The 10.1 cm (4 in) diameter flow loops are 30 m in length and are horizontally leveled. The test sections, where the measurements are taken, are located at least 8 m downstream from the exit of the pump or blower. The test sections (Figure 1) are 1.5 m long pipe spool pieces. Each has up to eight probe ports (four at the top, four at the bottom).

The experiments were carried out in multiphase, stratified flow with water and a mixture of CO<sub>2</sub>/N<sub>2</sub>/H<sub>2</sub>S. The tank is first filled with 1 m<sup>3</sup> of deionized water. Carbon dioxide (CO<sub>2</sub>) (and nitrogen in some cases) is injected in the loop at a specific pressure. The liquid phase is then heated up to the specific temperature by two electrical resistance heaters. The pump is started and the gas/liquid mixture is directed

<sup>(1)</sup> UNS numbers are listed in *Metals and Alloys in the Unified Numbering System*, published by the Society of Automotive Engineers (SAE International) and cosponsored by ASTM International.



FIGURE 1. Test section of the  $H_2S$  loop.

around the loop in a stratified flow regime (superficial gas velocity  $[V_{sg}] = 5$  m/s, superficial liquid velocity  $[V_{sl}] < 0.05$  m/s). Deoxygenation is performed by depressurizing the mixture several times until the concentration of oxygen is less than 50 ppb, as measured using a colorimetric test kit on the flowing solution taken directly from the tank. Once the deoxygenation is complete, acetic acid and/or  $H_2S$  concentrations are adjusted to the required levels. The corrosion probes are then introduced under pressure at the test section and the experiment begins. A data acquisition device is used to measure the total pressure and the gas/liquid temperature continuously.

### Liquid Phase Specification

The liquid phase is made up exclusively from deionized water. No salt is added. However, dissolved ferrous iron,  $Fe^{2+}$ , buildup occurs during the test as a

result of the corrosion process on the weight-loss (WL) specimens. Data on the evolution of the  $Fe^{2+}$  concentration and pH during the whole duration of the tests are shown in Table 1. It is important to mention that there may be some level of inaccuracy in the measurements, especially in the  $Fe^{2+}$  concentration because the liquid samples had to be diluted several times before testing. In the same way, a relative change of  $\pm 0.2$  unit in pH should be considered within the error of measurement. Samples of condensed liquid and in situ pH measurements were taken at the test section.

### Acetic Acid Concentration

The acetic acid concentration is adjusted by adding a calculated amount of glacial acetic acid in the tank. The acetic acid is first deoxygenated before being injected into the system using a high-pressure vessel connected to the tank. Several liquid samples are collected for analysis through an ion chromatograph to verify the concentration of total acetate species (free HAc +  $Ac^-$ ) introduced in the liquid phase. A differentiation is made between the free or undissociated acetic acid concentration (free HAc) and the total acetic acid concentration, which includes all acetate-containing species (free HAc and acetate  $Ac^-$ ). To keep the concentration of free acetic acid constant during the test, the pH of the liquid phase was adjusted (maintained constant), if necessary, by adding small amounts of glacial acetic acid. It should be noted that if the iron concentration increases and the pH is maintained constant by adding HAc, the free HAc concentration will change during the exposure.

Table 2 presents the calculated free acetic concentration at the bottom of the line for each test. The concentration of acetic acid was not measured at the top of the line, but it has been reported that the concentration of free acetic acid at the bottom of the line should be very similar to the concentration of total

TABLE 1  
Experimental Conditions

Duration	Acetic Acid Series						H <sub>2</sub> S Series						Acetic Acid/H <sub>2</sub> S Series					
	Test 1		Test 2		Test 3		Test 4		Test 5		Test 6		Test 7		Test 8		Test 9	
	pH	Fe <sup>2+</sup> ppm	pH	Fe <sup>2+</sup> ppm	pH	Fe <sup>2+</sup> ppm	pH	Fe <sup>2+</sup> ppm	pH	Fe <sup>2+</sup> ppm	pH	Fe <sup>2+</sup> ppm	pH	Fe <sup>2+</sup> ppm	pH	Fe <sup>2+</sup> ppm	pH	Fe <sup>2+</sup> ppm
At start	N/A	N/A	3.4	N/A	N/A	N/A	4.2	7.9	4.3	9	4.4	6.5	4.8	40	4.4	56.3	3.9	76
After 2 days	4.6	0.4	N/A	N/A	3.9	70	4.4	19	4.4	N/A	4	25	N/A	N/A	4.2	145	4.3	94
After 7 days	4.9	8.4	N/A	10	3.6	40	4.4	19	4.5	N/A	4.1	23	4.7	N/A	4.5	110	4.3	N/A
After 14 days	4.6	11	4	24	3.7	36	4.6	N/A	4.4	18	4.3	25	4.7	70	4.5	150	4.1	170
After 21 days	4.8	11	4	17	3.7	32	4.7	18	4.5	20	4.3	26	4.7	35	4.6	170	4.3	140

Notes: pH and  $Fe^{2+}$  measurements were taken from the bulk liquid phase in the tank. They do not represent the chemistry in the condensed liquid. N/A: Not available.

**TABLE 2**  
Acetic Acid Concentration

Test No.	Measured Total Acetate Species ([Free HAc] + [Ac <sup>-</sup> ]) in the Liquid Phase with Ion Chromatograph (ppm)	Calculated Free Acetic Acid Concentration in the Liquid Phase at the Bottom of the Line (ppm)	
		Based on the Amount of Acetate Species Measured with Ion chromatography	Based on the Amount of Acetate Species Introduced in the Experimental Loop
2	57	Between 50 and 55	Between 87 and 96
3	675	Between 605 and 664	Between 895 and 944
7	N/A	N/A	Between 46 and 57
8	1,052	Between 656 and 846	Between 630 and 810
9	1,120	Between 861 and 1,002	Between 772 and 895

acetate species (free HAc + Ac<sup>-</sup>) in the condensed liquid.<sup>13</sup> It is important to note that the concentration of free acetic acid injected into the tank is close to the concentration measured from the liquid at the bottom of the line by ion chromatograph, but in most cases a 20% to 30% discrepancy exists. This discrepancy is most likely the result of the technical difficulties often not only met in large-scale loop tests that target a high degree of accuracy in the measurements, but also errors possibly made in the measurement process. For clarity purposes, the concentration of free acetic acid will be displayed as 100 ppm or 1,000 ppm (depending on the test conditions) in this paper.

### Gas Phase Composition

In all of the experiments, the gas phase comprised a mixture of CO<sub>2</sub> and N<sub>2</sub> (2 bars of CO<sub>2</sub> and 0.7 bars of N<sub>2</sub>, 0.3 bars of water vapor) for a total pressure of 3 bars. For the H<sub>2</sub>S environment, the required amount of H<sub>2</sub>S was introduced in pure gas form at the beginning of the test and checked regularly using a piston pump and low-range standard detection tubes. The trace amounts of H<sub>2</sub>S introduced in the loop were consumed fairly rapidly by the corrosion process, and the H<sub>2</sub>S partial pressure had to be adjusted almost every day to maintain an accuracy of ±20%.

### Materials Characterization

All the weight-loss specimens are made of API<sup>(2)</sup> 5L X65 carbon steel prepared from the same piece of field pipe line. The chemical analyses of this X65 steel, its microstructure, and its hardness have been reported elsewhere.<sup>22</sup>

### Condensation Rate Measurement

Vapor phase condensation on the internal pipe wall was achieved by cooling specific segments of the loop (test sections) using copper tubing coiled around the outside of the pipe. Tap water was circulated through the coils and the flow rate was adjusted to reach the required amount of cooling. The condensa-

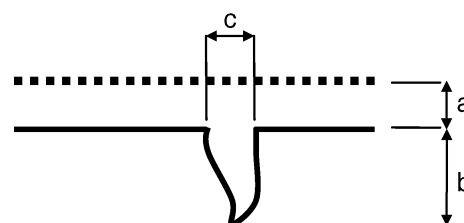


**FIGURE 2.** Schematic representation of pitting corrosion: (a) general corrosion depth, (b) pit depth after film removal, and (c) diameter of pit after film removal.

tion rate was measured either by using a water trap downstream of the test section or by measuring the difference of temperature between the gas and the pipe wall inner surface. A more detailed presentation of the cooling system has been published previously by the authors.<sup>8-10</sup>

### Localized Corrosion Characterization

Information on the occurrence and extent of localized corrosion was collected for each test performed using a 3D surface profilometer. It is therefore important to define clearly the parameters measured. For this purpose, the ASTM G46<sup>26</sup> standard for pitting corrosion was consulted, but no satisfactory guideline could be applied directly to the present study. Consequently, using the ASTM standard as a basis, the authors developed their own criteria for localized corrosion evaluation.

**Definition of Pitting Corrosion** — Generally, pits are deep and narrow, and either hemispherical or cup-shaped. When pitting corrosion happens, a part of the material surface undergoes rapid attack while most of the adjacent surface remains unaffected. As described in Figure 2, the criteria used to define pitting corrosion are displayed below:

- the pit depth is 5 times bigger than the general corrosion depth ( $b \geq 5a$ )
- the diameter of the pit after film removal is smaller than the pit depth ( $c \leq b$ )

**Definition of Mesa Attack** — Mesa attack is characterized by a wide and often flat-bottomed local

<sup>(2)</sup> American Petroleum Institute (API), 1220 L St. NW, Washington, DC, 20005.

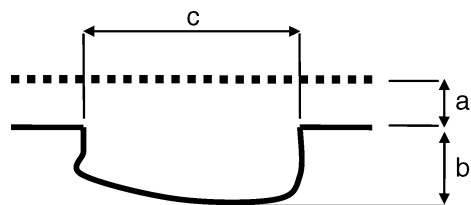


**FIGURE 3.** Schematic representation of mesa attack: (a) general corrosion depth, (b) pit depth after film removal, and (c) diameter of pit after film removal.

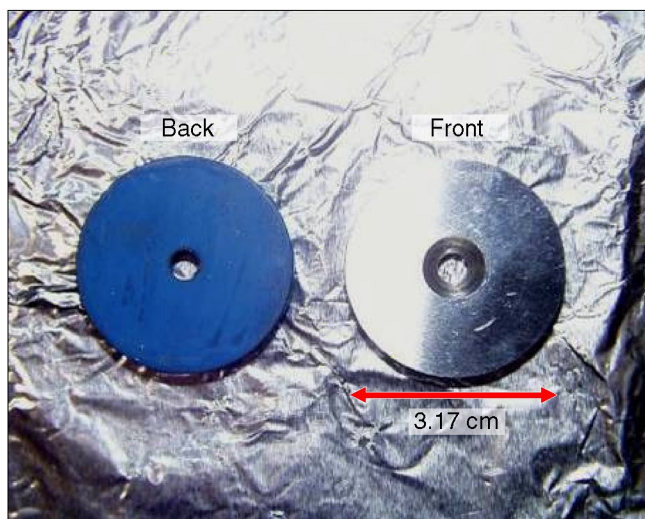


**FIGURE 4.** Weight-loss specimens as prepared using PTFE coating on the back and the side.

attack without protective corrosion film, surrounded by areas with intact corrosion films. Generally, mesa attack starts as several small pits growing beneath the porous corrosion film. These pits then can continue to grow beneath the corrosion film until the lid of the corrosion film is torn away by the mechanical forces of flow. Growth of the pits continues by corrosion, both laterally and in depth, then the original corrosion film is removed stepwise by the flow. Several such pits can be initiated during a short period of time and grow together into a wide, flat-bottomed mesa attack. A galvanic effect between the film-free corroding metal in the bottom of the mesa attack and the film-covered steel outside the mesa attack can increase the corrosion rate in the mesa attack area. As described in Figure 3, the criteria used for mesa attack are:

- the mesa attack depth is 5 times bigger than general corrosion depth ( $b \geq 5a$ )
- the diameter of mesa is bigger than pit depth ( $c \geq b$ )

*Percentage of Specimen Surface Affected by Localized Corrosion* — Since mild steel weight-loss specimens were used in this study, it was found that the percentage of the specimen surface affected by local-

ized corrosion (pitting and mesa attack together) constituted a likely indication of its occurrence.

### Corrosion Rate Measurement

The corrosion rates were measured using weight-loss specimens made of X65 carbon steel. The weight-loss specimens were not inserted into the corrosion environment until the system had reached steady state (stable temperature, pressure, and flow velocities). Weight-loss specimens are circular disks with a central mounting hole (0.76 cm internal diameter, 3.17 cm external diameter, and 0.5 cm thickness) and an exposed area of 7.44 cm<sup>2</sup>, which were polished using isopropanol (C<sub>3</sub>H<sub>8</sub>O) as a coolant on silicon carbide (SiC) papers, up to 600 grit. After this preparation, they were covered with liquid polytetrafluoroethylene (PTFE) on the outer edges and bottom. Following 4 h to 6 h of curing at ambient conditions, the PTFE-coated specimens were held at 200°C in an oven for 4 h. After cooling, the uncovered steel surface was then repolished with 600-grit SiC paper wetted with isopropanol; finally, the specimen was cleaned, dried, and weighed. The specimen after preparation is shown in Figure 4. The specimens were then flush-mounted on the internal pipe wall of the loop by using a specially designed probe holder, meaning only one face of the specimen was in direct contact with the corrosive environment. The exposure time was between 2 days and 21 days. Upon removal from the loop, the specimen surface was flushed with isopropanol to dehydrate it; photographs of the surface were then taken. The weight of the specimen after each test was registered, and the ASTM G1<sup>27</sup> standard procedure was followed to remove the corrosion products and to determine the corrosion rate by weight loss.

One specimen is used generally for weight loss, and the other is preserved for corrosion product evaluation using scanning electron microscopy (SEM) and energy-dispersion analysis (EDS).

### Test Matrix

Table 3 presents the experimental conditions of each test. Only two parameters (free acetic acid concentration and H<sub>2</sub>S partial pressure) were varied around a set of baseline conditions (Test 1). The influence of these two parameters were studied separately (Tests 2 through 6) and then combined in Tests 7, 8, and 9. More information about the test conditions has been reported previously.<sup>22</sup>

The nine experiments conducted to investigate different aspects of the corrosion process in a CO<sub>2</sub> environment can be divided into three groups:

- influence of the concentration of free acetic acid
- influence of the partial pressure of H<sub>2</sub>S
- combined effect of the concentration of free acetic acid and the partial pressure of H<sub>2</sub>S

Apart from the acetic acid concentration and the partial pressure of H<sub>2</sub>S, all the other experimen-

**TABLE 3**  
Test Matrix

Experiment no.	1	2	3	4	5	6	7	8	9
Investigating	Acetic Acid			H <sub>2</sub> S			Acetic Acid/H <sub>2</sub> S		
Free HAC tank (ppm)	0	100	1,000	0	0	0	100	1,000	1,000
pH <sub>2</sub> S (bar)	0	0	0	0.004	0.07	0.13	0.004	0.004	0.13

Common parameters—Steel type: X65; Liquid phase composition: DI water; Test duration: 3 weeks; Absolute pressure: 3 bars; pCO<sub>2</sub>: 2 bars; Gas temperature: 70°C; Gas velocity: 5 m/s; Water condensation rate (WCR): 0.25 mL/m<sup>2</sup>/s; Superficial liquid velocity < 0.05 m/s.

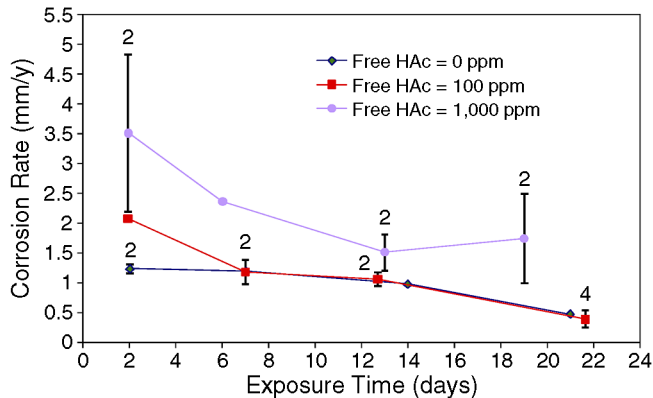


**FIGURE 5.** Influence of the free HAC concentration. Evolution of the general corrosion rate over time. (Total pressure [ $P_T$ ]: 3 bars, CO<sub>2</sub> partial pressure [ $p_{CO_2}$ ]: 2 bars, H<sub>2</sub>S partial pressure [ $p_{H_2S}$ ]: 0 bar, gas temperature [ $T_g$ ]: 70°C, water condensation rate [WCR]: 0.25 mL/m<sup>2</sup>/s, gas velocity [ $V_g$ ]: 5 m/s).

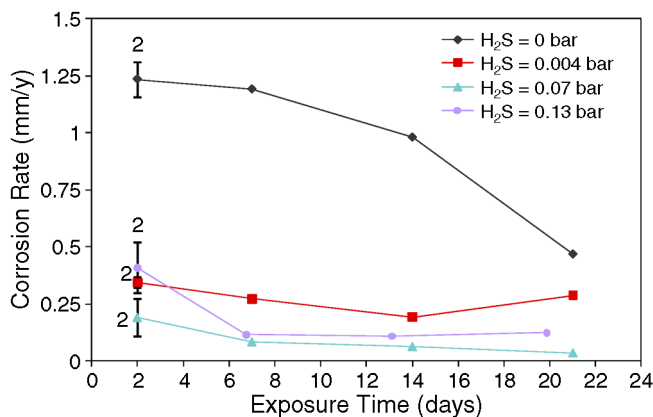


**FIGURE 7.** Influence of the partial pressure of H<sub>2</sub>S. Evolution of the general corrosion rate with the partial pressure of H<sub>2</sub>S. ( $P_T$ : 3 bars, pCO<sub>2</sub>: 2 bars, free HAC: 0 ppm,  $T_g$ : 70°C, WCR: 0.25 mL/m<sup>2</sup>/s,  $V_g$ : 5 m/s).

tal parameters were kept at fixed values (system temperature: 70°C, partial pressure of CO<sub>2</sub>: 2 bars, total pressure: 3 bars, gas velocity: 5 m/s, water condensation rate: 0.25 mL/m<sup>2</sup>/s).

## CORROSION RATE RESULTS

Corrosion rate results are displayed in a series of plots in Figures 5 through 14. In addition to the evolution of the average (uniform) corrosion rate with

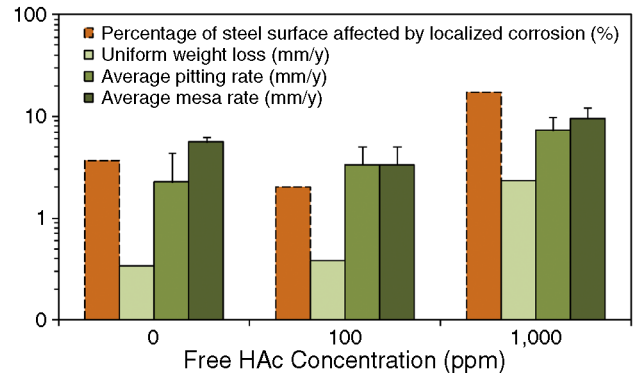


**FIGURE 6.** Localized corrosion – Influence of the free HAC concentration in pure CO<sub>2</sub> environment. ( $P_T$ : 3 bars, pCO<sub>2</sub>: 2 bars, pH<sub>2</sub>S: 0 bar,  $T_g$ : 70°C, WCR: 0.25 mL/m<sup>2</sup>/s,  $V_g$ : 5 m/s, exposure time: 21 days).

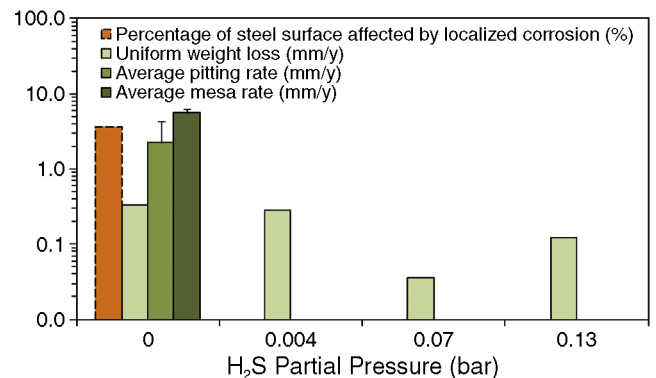


**FIGURE 8.** Localized corrosion – Influence of the H<sub>2</sub>S partial pressure. ( $P_T$ : 3 bars, pCO<sub>2</sub>: 2 bars, free HAC: 0 ppm,  $T_g$ : 70°C, WCR: 0.25 mL/m<sup>2</sup>/s,  $V_g$ : 5 m/s, exposure time: 3 weeks).

time, key data about the occurrence of localized corrosion are displayed. The graphs present corrosion rates from pitting or mesa attack and they also indicate the percentage of surface area of the specimen affected by localized corrosion (pitting or mesa). The corresponding values were obtained by performing a surface analysis on each specimen with a 3D surface profilometer. The average (uniform) corrosion rate was calculated using the weight loss of a specimen and the time of exposure. Error bars representing the maximum and minimum values, and the number of specimens (number of repeated measurements) are displayed where applicable on each graph.

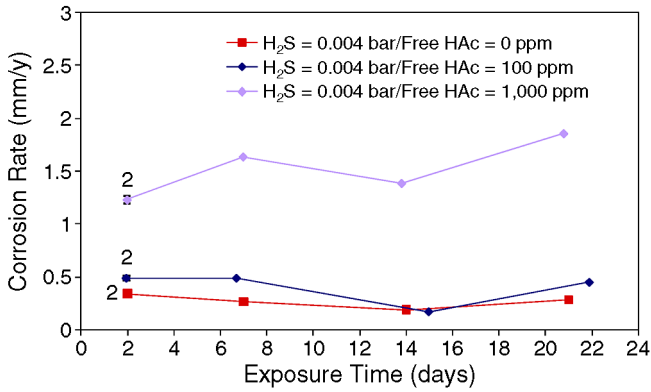


**FIGURE 9.** Combined effect of the partial pressure of  $H_2S$  and the concentration of free HAc. Evolution of the general corrosion rate over time. ( $P_T$ : 3 bars,  $pCO_2$ : 2 bars,  $pH_2S$ : 0.004 bar,  $T_g$ : 70°C, WCR: 0.25 mL/m<sup>2</sup>/s,  $V_g$ : 5 m/s).

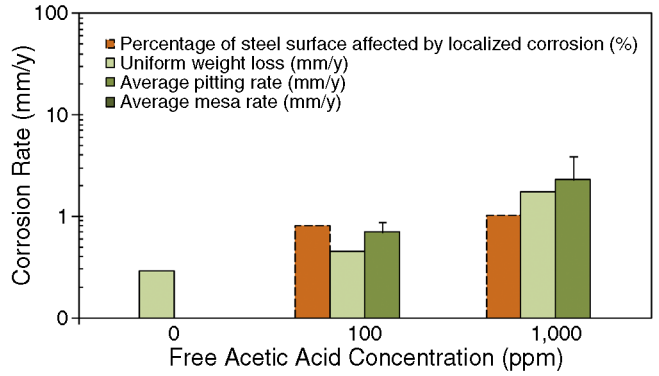


**FIGURE 10.** Localized corrosion – Influence of the free HAc concentration in  $CO_2/H_2S$  environment. ( $P_T$ : 3 bars,  $pCO_2$ : 2 bars,  $pH_2S$ : 0.004 bar,  $T_g$ : 70°C, WCR: 0.25 mL/m<sup>2</sup>/s,  $V_g$ : 5 m/s, exposure time: 3 weeks).

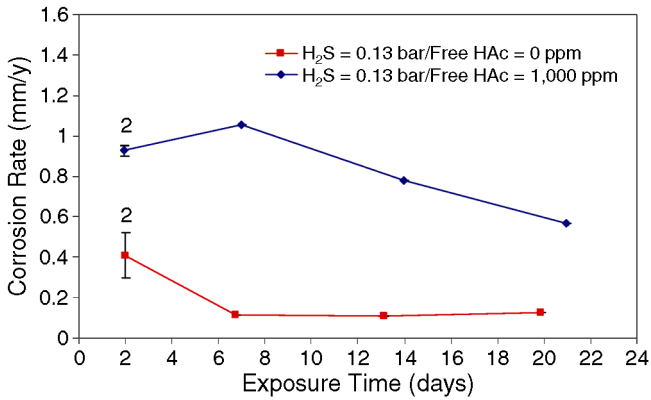


**FIGURE 11.** Combined effect of the partial pressure of  $H_2S$  and the concentration of free HAc. Evolution of the general corrosion rate over time. ( $P_T$ : 3 bars,  $pCO_2$ : 2 bars,  $pH_2S$ : 0.13 bar,  $T_g$ : 70°C, WCR: 0.25 mL/m<sup>2</sup>/s,  $V_g$ : 5 m/s).

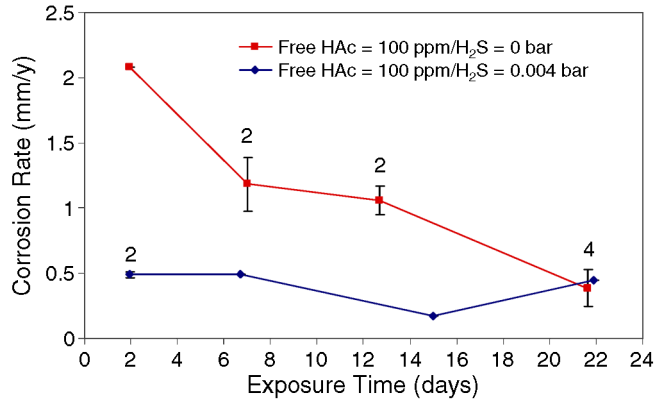


**FIGURE 12.** Combined effect of the partial pressure of  $H_2S$  and the concentration of free HAc. Evolution of the general corrosion rate over time. ( $P_T$ : 3 bars,  $pCO_2$ : 2 bars, free HAc: 100 ppm,  $T_g$ : 70°C, WCR: 0.25 mL/m<sup>2</sup>/s,  $V_g$ : 5 m/s).

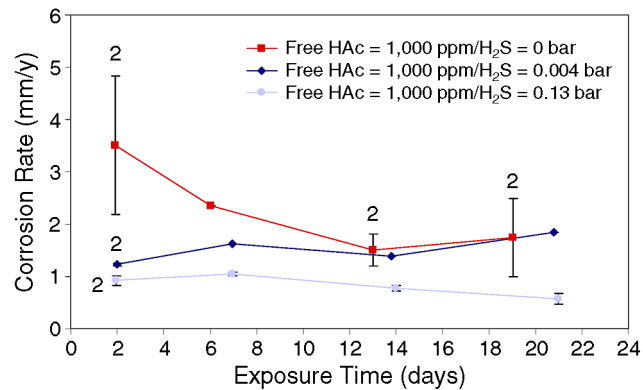


**FIGURE 13.** Combined effect of the partial pressure of  $H_2S$  and the concentration of free HAc. Evolution of the general corrosion rate over time. ( $P_T$ : 3 bars,  $pCO_2$ : 2 bars, free HAc: 1,000 ppm,  $T_g$ : 70°C, WCR: 0.25 mL/m<sup>2</sup>/s,  $V_g$ : 5 m/s).

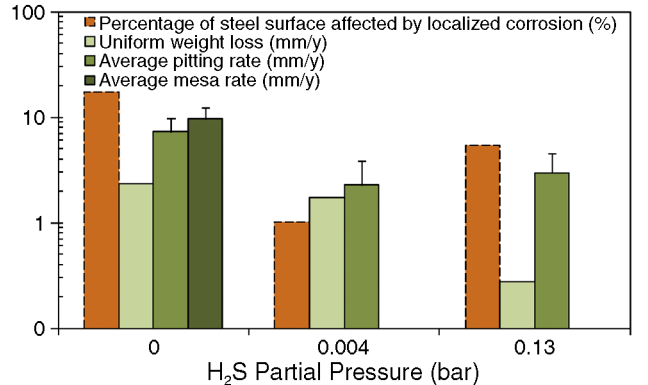


**FIGURE 14.** Localized corrosion – Influence of the free HAc concentration in  $CO_2/H_2S$  environment. ( $P_T$ : 3 bars,  $pCO_2$ : 2 bars, free HAc: 1,000 ppm,  $T_g$ : 70°C,  $V_g$ : 5 m/s, WCR: 0.25 mL/m<sup>2</sup>/s, exposure time: 3 weeks).

### *Influence of the Free Acetic Acid Concentration*

The influence of the concentration of free acetic acid on the corrosion rate at the top of the line is shown in Figures 5 and 6. The effect of 100 ppm of free acetic acid seems negligible, but 1,000 ppm free acetic acid almost doubles the general corrosion rate over the test exposure time. In addition, while pure CO<sub>2</sub> TLC rates tend to decrease rapidly with time because of the formation of a protective FeCO<sub>3</sub> layer, the corrosion rate with 1,000 ppm of free acetic acid remains almost constant at 2 mm/y after 3 weeks of testing. Moreover, the presence of acetic acid strongly promotes the occurrence of pitting corrosion as the maximum mesa/pitting rate was measured at more than 12 mm/y after 3 weeks of testing. It can be stated that the occurrence of pitting corrosion is proportional to the amount of free acetic acid in the solution. The continuous renewal of condensed droplets made more corrosive by the presence of acid acetic vapor is believed to be responsible for the breakdown of corrosion product layer protectiveness.

### *Influence of the Partial Pressure of Hydrogen Sulfide*

Figures 7 and 8 present information about general and localized corrosion in environments containing H<sub>2</sub>S, but no acetic acid. The presence of trace amounts of H<sub>2</sub>S (pH<sub>2</sub>S = 0.04 bar, CO<sub>2</sub>/H<sub>2</sub>S ratio = 500) clearly decreased the corrosion rate as compared to a pure CO<sub>2</sub> environment. This is generally explained by the formation of a very protective film of iron sulfide on the surface of the metal. It is expected that further additions of H<sub>2</sub>S (pH<sub>2</sub>S up to 0.13 bar, CO<sub>2</sub>/H<sub>2</sub>S ratio: 15) should cause a gradual increase in the corrosion rate. This is not obviously the case at the top of the line where it is difficult to identify a distinct trend. The additional cathodic reaction may compete with an increase in protectiveness of the iron sulfide film. It seems, however, that the corrosion decreases rapidly in the first 15 days and then reverses this tendency and increases slightly. One of the main differences with a pure CO<sub>2</sub> environment is that the corrosion process does not seem to slow down considerably, even if the severity of the attack is lower. No localized corrosion (pitting or mesa attack) was observed at the top of the line in the conditions tested.

### *Combined Effect of Acetic Acid and Hydrogen Sulfide*

The influence of acetic acid on H<sub>2</sub>S TLC is shown in Figures 9 through 14. As in a CO<sub>2</sub>/H<sub>2</sub>S environment, the TLC rates remained more or less constant during the entire duration of the test. While 100 ppm of free acetic acid seems to have little effect, the corrosion rate jumps from 0.3 mm/y to 1.8 mm/y with 0.004 bar of H<sub>2</sub>S when 1,000 ppm of the weak acid is present. It is interesting to note that, with traces of

H<sub>2</sub>S (pH<sub>2</sub>S = 0.004 bar, CO<sub>2</sub>/H<sub>2</sub>S ratio: 500), the average TLC rate after 21 days of exposure is similar to the one obtained in pure CO<sub>2</sub> environment when a significant amount of free acetic acid is present (Figure 13). Further increases in H<sub>2</sub>S partial pressure (0.13 bar of H<sub>2</sub>S, CO<sub>2</sub>/H<sub>2</sub>S ratio: 15) seem to reverse this tendency and offer better protection against TLC. The average corrosion rate after 3 weeks of exposure is still three to four times higher with 1,000 ppm of acetic acid than without it.

In the presence of acetic acid, some localized corrosion was observed, but only in the form of small pits. The percentage area affected by pitting corrosion is usually very limited (unlike in a pure CO<sub>2</sub> environment) and pitting rates do not exceed 4 mm/y, which barely qualifies the corrosion as pitting in accordance with what was learned in the procedure presented earlier.

## SURFACE ANALYSIS

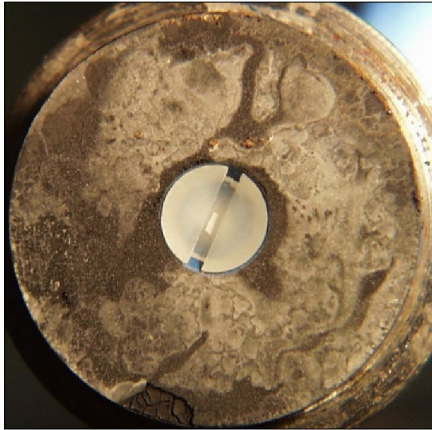
The corrosion product layer for each test was systematically studied using SEM, EDS, and a 3D surface profilometer. Visual observations obtained with SEM give useful indications about the nature of the corrosion product film, but some caution should be taken when interpreting these observations because of the lack of XRD analysis. It is very likely that the corrosion product scale produced in this sour environment is made mainly of mackinawite, though cubic FeS and/or triolite (long, flower-shaped crystals) have been experienced in similar experimental conditions.

### *Influence of the Free Acetic Acid Concentration*

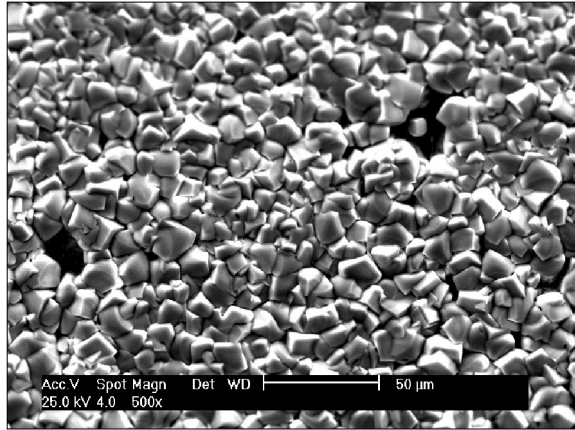
The surface analysis associated with the influence of acetic acid on CO<sub>2</sub> TLC is shown in Figures 15 and 16. A protective FeCO<sub>3</sub> film usually forms at the metal surface when supersaturation conditions are reached in the droplet of condensed water (high pH associated with high Fe<sup>2+</sup> concentration). The presence of high concentrations of free acetic acid (1,000 ppm of free acetic acid at the bottom of the line) clearly affects the relative protectiveness of the scale by decreasing the pH of the freshly condensed liquid (local acidification leading to some FeCO<sub>3</sub> dissolution) and by adding another cathodic reaction. Numerous breakdowns of the layer are seen all over the specimen surface. Localized corrosion occurs through pitting and mesa attacks.

### *Influence of the Partial Pressure of Hydrogen Sulfide*

SEM and EDS analyses of the corrosion layer formed in CO<sub>2</sub>/H<sub>2</sub>S environments without acetic acid are shown in Figure 17 (pH<sub>2</sub>S = 0.004 bar, CO<sub>2</sub>/H<sub>2</sub>S ratio: 500) and Figure 18 (pH<sub>2</sub>S = 0.13 bar, CO<sub>2</sub>/H<sub>2</sub>S ratio: 15). In all cases, even though the tests were performed with 2 bars of CO<sub>2</sub>, no FeCO<sub>3</sub> crystals could be



(a) WL specimen after 21 days of exposure.

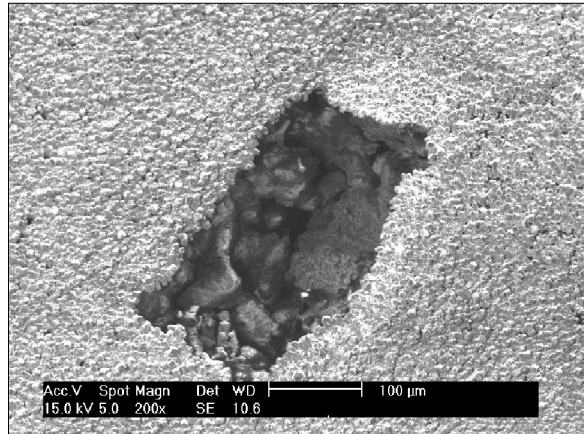


(b) Corrosion product layer, X500.

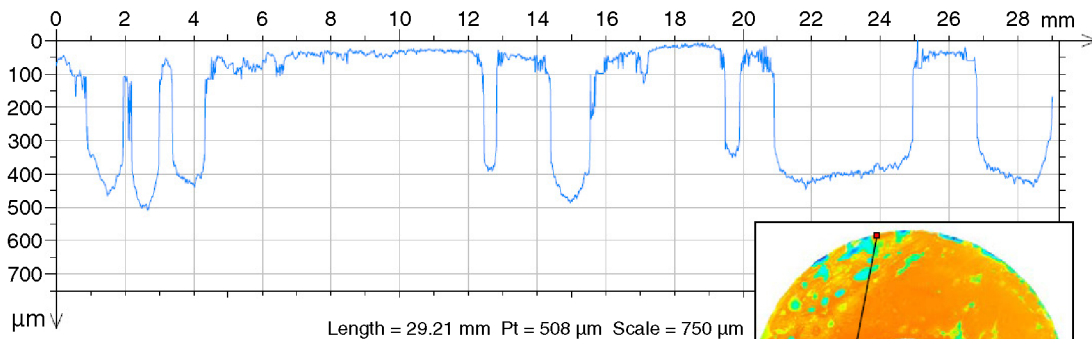
**FIGURE 15.** Test 1 – Pure  $\text{CO}_2$  environment. ( $p\text{CO}_2$ : 2 bars,  $p\text{H}_2\text{S}$ : 0 bar, free HAc: 0 ppm,  $T_g$ : 70°C,  $V_g$ : 5 m/s, WCR: 0.25 mL/m<sup>2</sup>/s, exposure time: 3 weeks).



(a) WL specimen after 21 days of exposure.



(b) Corrosion product layer, X200.



(c) Profilometer analysis after removal for the corrosion product layer.

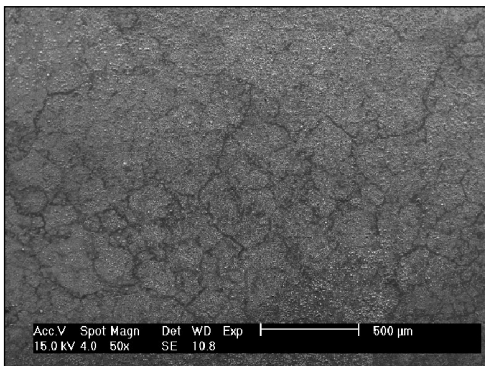
**FIGURE 16.** Test 3 – Pure  $\text{CO}_2$  environment with acetic acid. ( $p\text{CO}_2$ : 2 bars, no  $\text{H}_2\text{S}$ , free HAc: 1,000 ppm,  $T_g$ : 70°C, WCR: 0.25 mL/m<sup>2</sup>/s,  $V_g$ : 5 m/s, exposure time: 3 weeks).



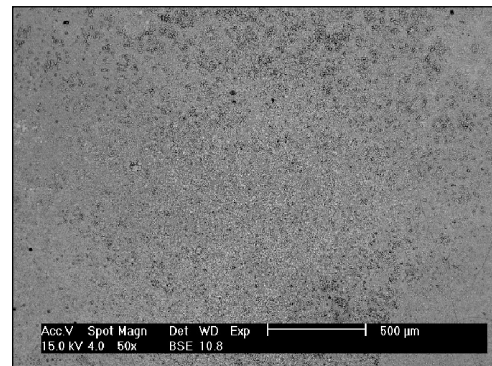
(a) WL specimen after 21 days of exposure.



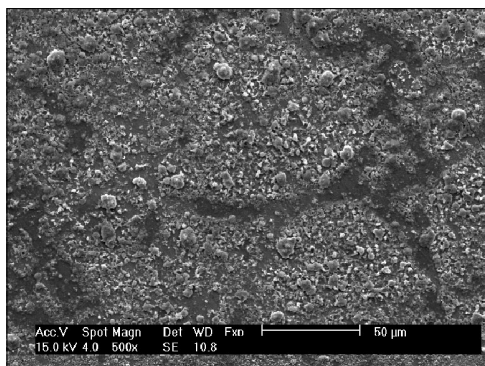
(b) WL specimen after removal of the layer.



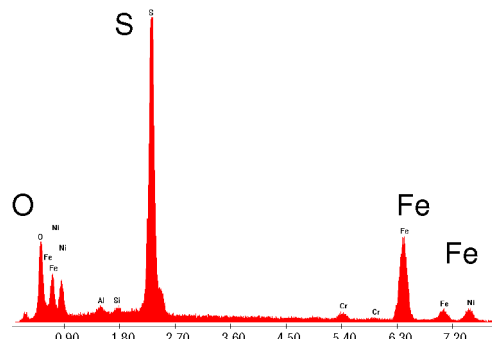
(c) Corrosion product layer, X50.



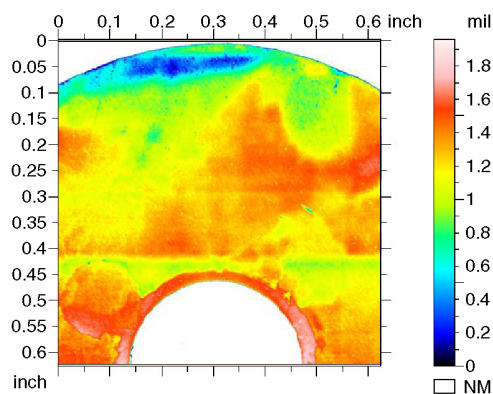
(d) Corrosion product, X50, back scatter.



(e) Corrosion product layer, X500.



(f) EDS analysis of the corrosion layer e.



(g) Profilometer analysis after removal for the corrosion product layer.

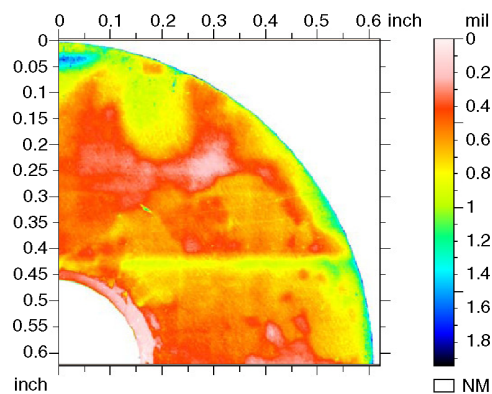
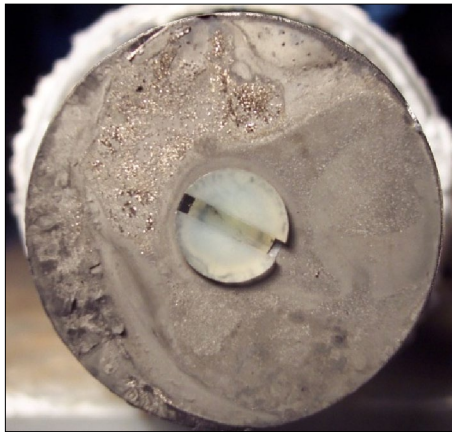


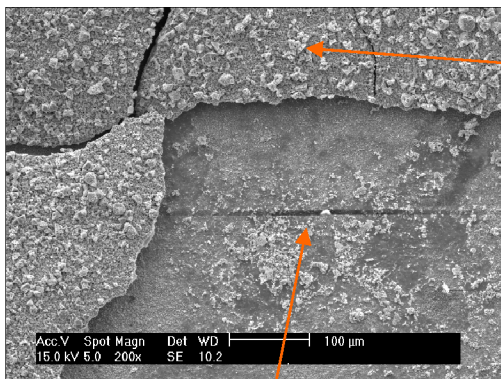
**FIGURE 17.** Test 4 –  $\text{CO}_2$  environment with traces of  $\text{H}_2\text{S}$  –  $\text{CO}_2/\text{H}_2\text{S}$ : 500. ( $p\text{CO}_2$ : 2 bars,  $p\text{H}_2\text{S}$ : 0.004 bar, no free HAC,  $T_g$ : 70°C, WCR: 0.25 mL/m<sup>2</sup>/s,  $V_g$ : 5 m/s, exposure time: 3 weeks).



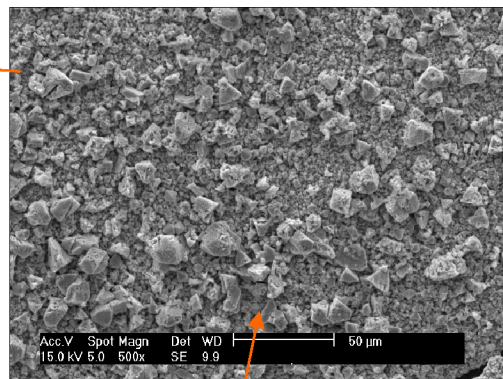
(a) WL specimen after 21 days of exposure.



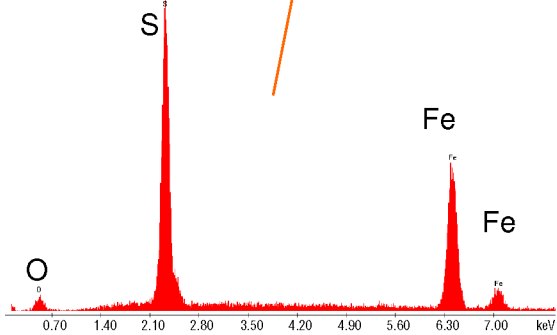
(b) WL specimen after removal of the layer.



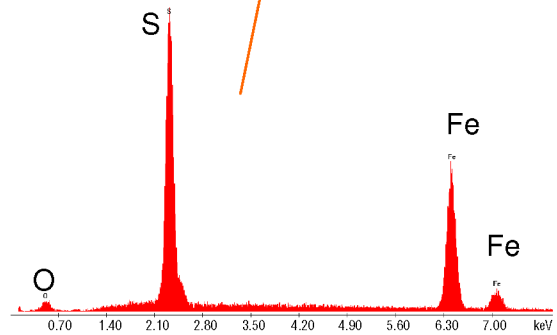
(c) Corrosion product layer, X200.



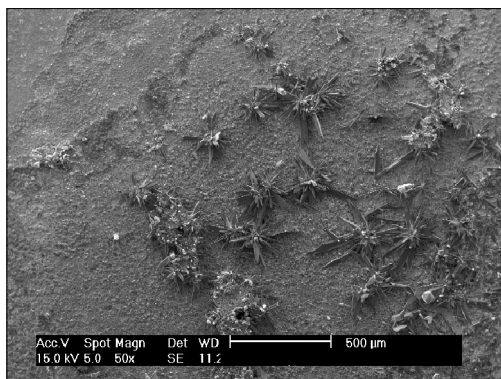
(d) Corrosion product layer, X500.



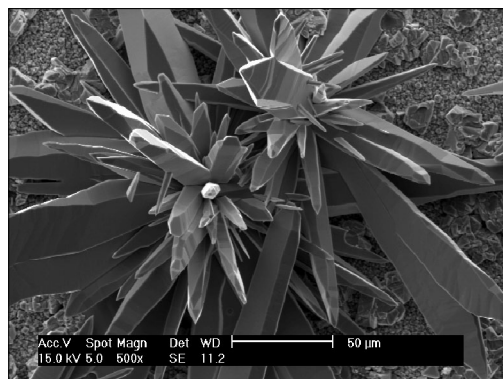
(e) EDS analysis of the corrosion layer c.



(f) EDS analysis of the corrosion layer d.



(g) Corrosion product layer, X50.



(h) Corrosion product layer, X500.

**FIGURE 18.** Test 6 –  $\text{CO}_2$  environment with  $\text{H}_2\text{S} - \text{CO}_2/\text{H}_2\text{S}$ : 15. ( $p\text{CO}_2$ : 2 bars,  $p\text{H}_2\text{S}$ : 0.13 bar, no free HAc,  $T_g$ : 70°C, WCR: 0.25 mL/m<sup>2</sup>/s,  $V_g$ : 5 m/s, exposure time: 3 weeks).

identified clearly (although their presence cannot be ruled out). Instead, a mostly macroscopically amorphous corrosion product layer covers the specimen surface. The layer does not always appear to be homogeneous, especially at higher H<sub>2</sub>S partial pressures where large parts of the product layer seem to have peeled off during the corrosion process. In addition, peculiar features (which show an obvious crystalline structure) could be observed but could not be identified clearly since EDS analysis always shows similar peaks of iron (Fe) and sulfide (S). In all cases, the steel was uniformly corroded and no localized corrosion could be observed even after 21 days of exposure to the corrosive environment.

### *Combined Effect of Acetic Acid and Hydrogen Sulfide*

The surface analysis associated with the influence of acetic acid on CO<sub>2</sub>/H<sub>2</sub>S TLC is shown in Figures 19 through 21. The corrosion product layer at the top of the line is made of FeS, which is usually the case at the top of the line in H<sub>2</sub>S environments. In all cases, the film looks fairly uniform, is quite porous, and is easily wiped off the surface of the specimen. The film is also, in most cases, cracked; this cracking is believed to take place over time because of the internal mechanical stress. The corrosion process then could continue under the film. FeCO<sub>3</sub> crystals could be observed in these cracks. There is no clear difference in the EDS analysis (identification of the film composition) performed for the tests with or without acetic acid. The surface looks evenly corroded except for a few isolated pits, especially at higher concentrations of acetic acid. Once again, the extent of localized corrosion seems to be negligible with maximum pitting rates close to average corrosion rates.

## CONCLUSIONS

### ❖ Influence of the Acetic Acid Concentration on CO<sub>2</sub> Top-of-the-Line Corrosion

- The presence of acetic acid increases the initial corrosion rate at the top of the line.
- In a CO<sub>2</sub> environment, the presence of significant concentrations of acetic acid strongly promotes localized corrosion. The effect seems to be proportional to the amount of acid present.

### ❖ Main Characteristics of H<sub>2</sub>S/CO<sub>2</sub> Top-of-the-Line Corrosion

- In the presence of H<sub>2</sub>S, the average corrosion rate at the top and the bottom of the line starts at a low value and remains relatively constant over time.
- The presence of trace amounts of H<sub>2</sub>S retards the average corrosion rate compared to a pure CO<sub>2</sub> environment. There is no clear influence of further additions of H<sub>2</sub>S (up to 0.13 bar) on the average corrosion rate.

—At the top of the line, no localized corrosion was observed in the presence of H<sub>2</sub>S (up to 0.13 bar) after 21 days of testing.

### ❖ Influence of the Presence of Acetic Acid on CO<sub>2</sub>/H<sub>2</sub>S Top-of-the-Line Corrosion

- In the presence of H<sub>2</sub>S, the presence of acetic acid seems to affect the integrity of the FeS film and strongly influences the general corrosion rate.
- The presence of acetic acid in sour conditions seems to trigger the occurrence of localized corrosion in the form of small pits. The maximum pitting rate measured falls close to the average corrosion rate and therefore is considered to be identical mechanisms.

## ACKNOWLEDGMENTS

The authors would like to express their gratitude to Total, BP, ConocoPhillips, Chevron, Occidental Oil Company, Saudi Aramco, and ENI for the financial support of this research and for allowing the publication of this paper. The authors are also grateful for the contributions of D. Hinkson, Z. Zhang, and V. Wang, colleagues at the Institute, to this experimental work. Finally, the authors are thankful to D. Young for his guidance and expertise on sulfide chemistry and H<sub>2</sub>S corrosion phenomena.

## REFERENCES

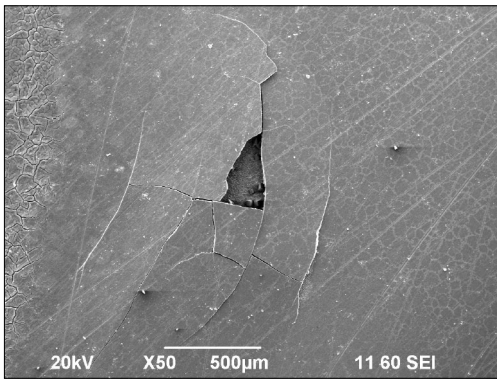
1. R. Paillassa, M. Dieumegard, M. Estevoyer, "Corrosion Control in the Gathering System at Lacq Sour Gas Field," in Proc. 2nd Int. Congress of Metallic Corrosion (Houston, TX: NACE International, 1963), p. 410-417.
2. Y. Gunaltun, D. Supriyataman, A. Jumakludin, "Top-of-the-Line Corrosion in Multiphase Gas Line. A Case History," CORROSION/1999, paper no. 36 (Houston, TX: NACE, 1999).
3. M. Thammachart, Y. Gunaltun, S. Punpruk, "The Use of Inspection Results for the Evaluation of Batch Treatment Efficiency and the Remaining Life of the Pipelines Subjected to Top-of-Line Corrosion," CORROSION/2008, paper no. 08471 (Houston, TX: NACE, 2008).
4. Y. Gunaltun, D. Larrey, "Correlation of Cases of Top-of-the-Line Corrosion with Calculated Water Condensation Rates," CORROSION/2000, paper no. 71 (Houston, TX: NACE, 2000).
5. D.F. Ho-Chung-Qui, A.I. Williamson, P. Eng, "Corrosion Experiences and Inhibition Practices in Wet Sour Gathering Systems," CORROSION/1987, paper no. 46 (Houston, TX: NACE, 1987).
6. M. Edwards, B. Cramer, "Top-of-the-Line Corrosion—Diagnostic, Root Cause Analysis and Treatment," in CORROSION/2000, paper no. 72 (Houston, TX: NACE, 2000).
7. R.L. Martin, "Control of Top-of-Line Corrosion in Sour Gas Gathering Pipeline with Corrosion Inhibitors," CORROSION/2009, paper no. 9288 (Houston, TX: NACE, 2009).
8. M. Singer, D. Hinkson, Z. Zhang, H. Wang, S. Nešić, "CO<sub>2</sub> Top-of-the-Line Corrosion in Presence of Acetic Acid—A Parametric Study," CORROSION/2009, paper no. 09292 (Houston, TX: NACE, 2009).
9. M. Singer, S. Nešić, Y. Gunaltun, "Top-of-the-Line Corrosion in Presence of Acetic Acid and Carbon Dioxide," CORROSION/2004, paper no. 04377 (Houston, TX: NACE, 2004).
10. C. Mendez, M. Singer, A. Camacho, S. Hernandez, S. Nešić, "Effect of Acetic Acid, pH, and MEG on the CO<sub>2</sub> Top-of-the-Line Corrosion," CORROSION/2005, paper no. 5278 (Houston, TX: NACE, 2005).
11. T. Andersen, A.M.K. Halvorsen, A. Valle, G. Kojen, A. Dugstad, "The Influence of Condensation Rate and Acetic Acid Concentration on TOL Corrosion in Multiphase Pipelines," CORROSION/2007, paper no. 07312 (Houston, TX: NACE, 2007).



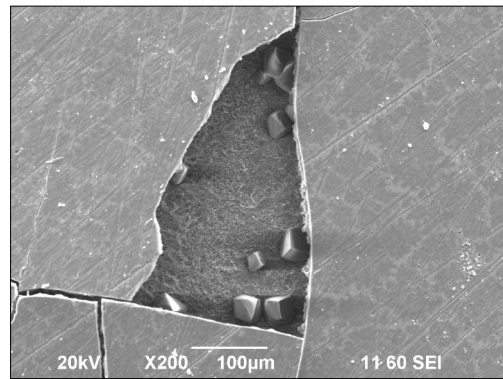
(a) WL specimen after 21 days of exposure.



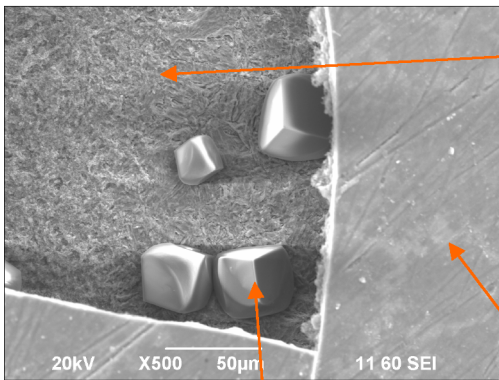
(b) WL specimen after removal of the layer.



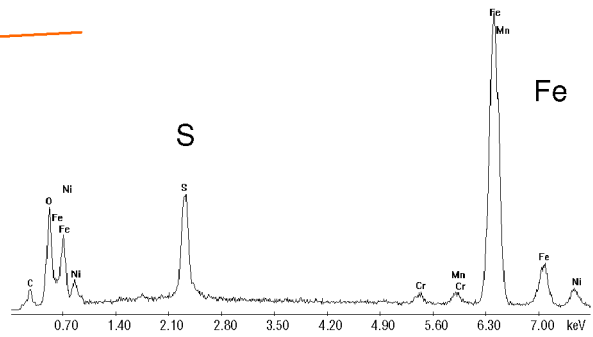
(c) Corrosion product layer, X50.



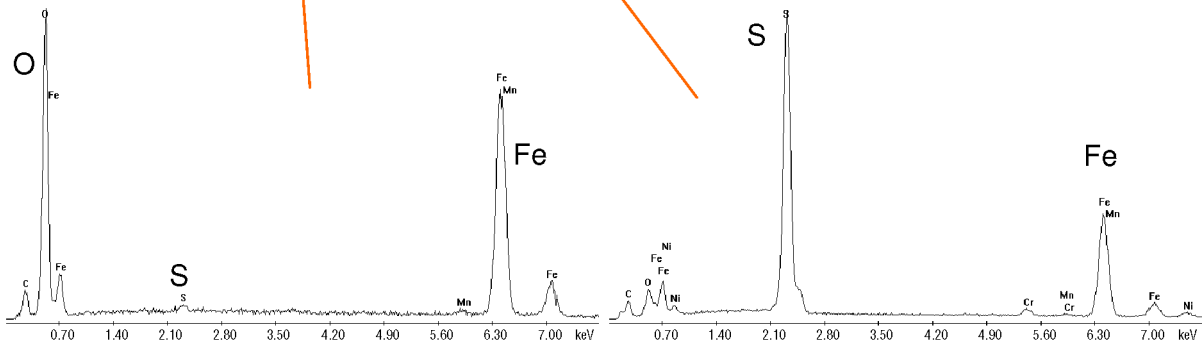
(d) Corrosion product layer, X200.



(e) Corrosion product layer, X500.



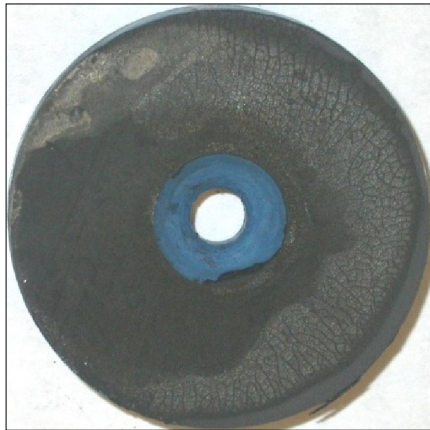
(f) EDS analysis of the corrosion layer e.



(g) EDS analysis of the corrosion layer e.

(h) EDS analysis of the corrosion layer e.

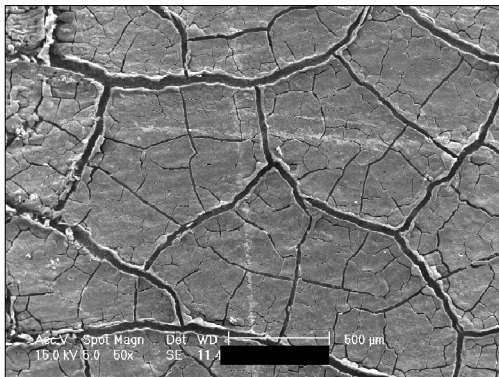
**FIGURE 19.** Test 7 – CO<sub>2</sub> environment with traces of H<sub>2</sub>S and acetic acid – CO<sub>2</sub>/H<sub>2</sub>S: 500. (pCO<sub>2</sub>: 2 bars, pH<sub>2</sub>S: 4 mbar, free HAC: 100 ppm, T<sub>g</sub>: 70°C, WCR: 0.25 mL/m<sup>2</sup>/s, V<sub>g</sub>: 5 m/s, exposure time: 3 weeks).



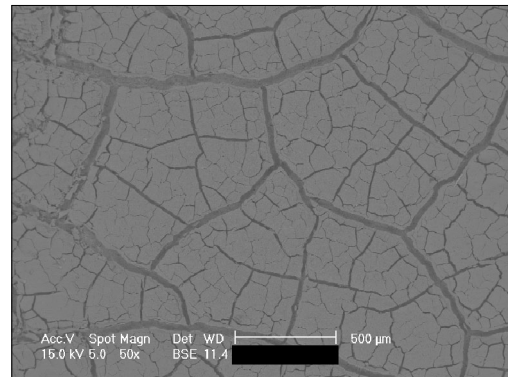
(a) WL specimen after 21 days of exposure.



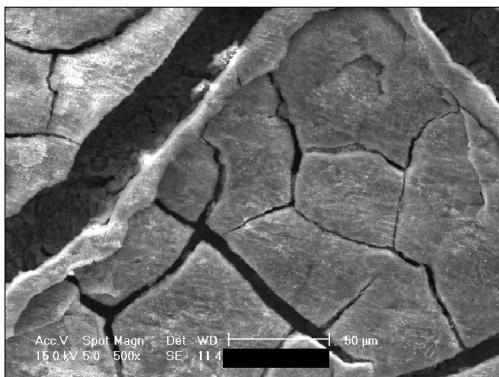
(b) WL specimen after removal of the layer.



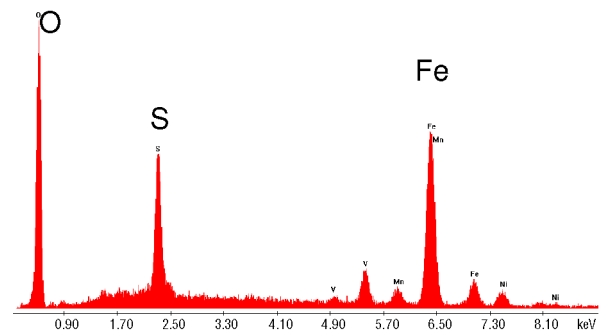
(c) Corrosion product layer, X100.



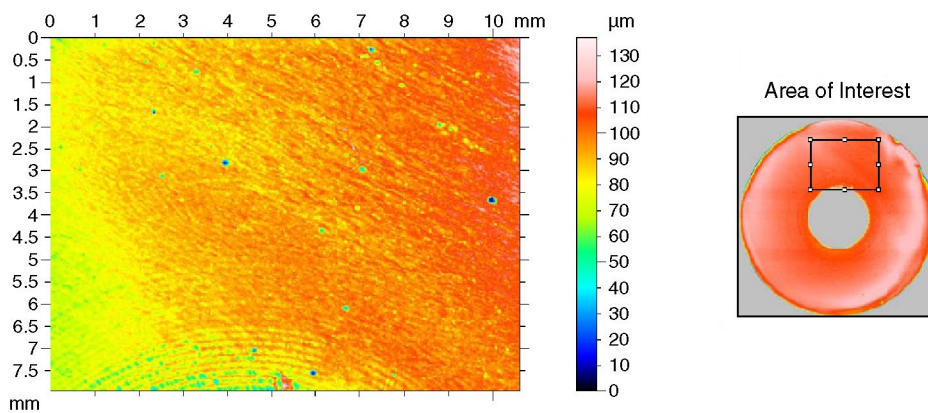
(d) Corrosion product, X50, back scatter.



(e) Corrosion product layer, X500.



(f) EDS analysis of the corrosion layer e.



(g) Profilometer analysis after removal for the corrosion product layer.

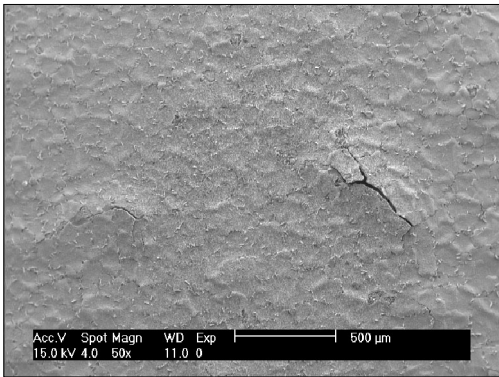
**FIGURE 20.** Test 8 –  $\text{CO}_2$  environment with traces of  $\text{H}_2\text{S}$  and acetic acid –  $\text{CO}_2/\text{H}_2\text{S}$ : 500.



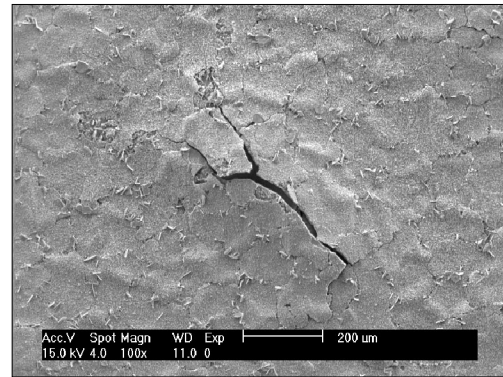
(a) WL specimen after 21 days of exposure.



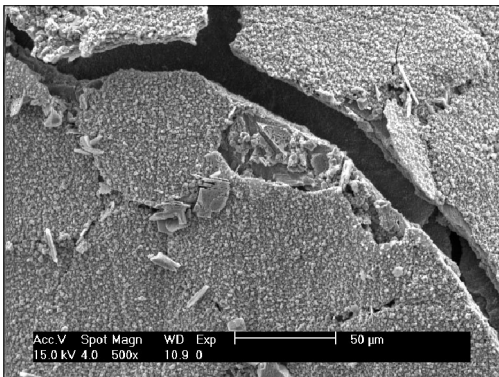
(b) WL specimen after removal of the layer.



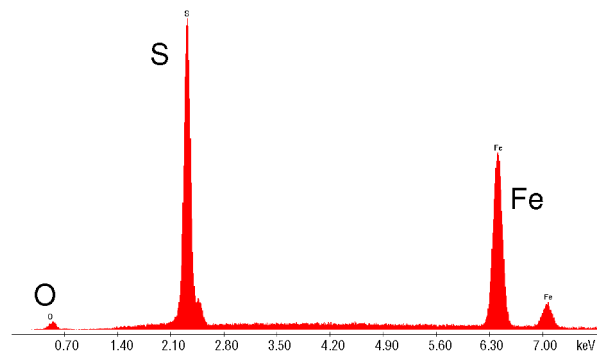
(c) Corrosion product layer, X50.



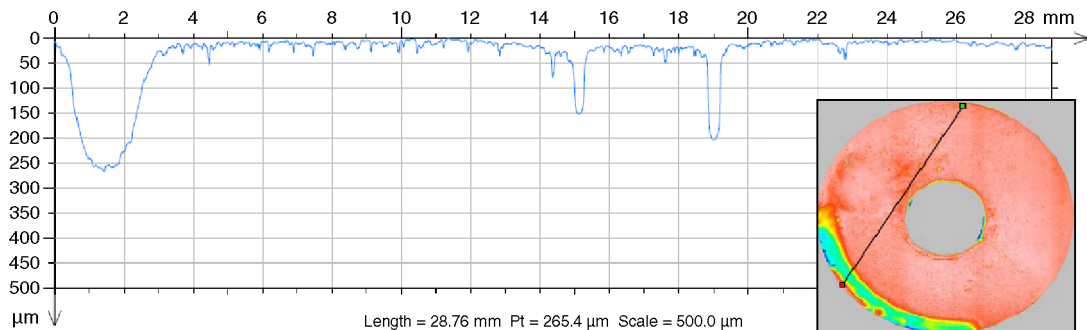
(d) Corrosion product layer, X100.



(e) Corrosion product layer, X500.



(f) EDS analysis of the corrosion layer e.



(g) Profilometer analysis after removal for the corrosion product layer.

Extracted profile

**FIGURE 21.** Test 9 –  $\text{CO}_2$  environment with  $\text{H}_2\text{S}$  and acetic acid –  $\text{CO}_2/\text{H}_2\text{S}$ : 15. ( $\text{pCO}_2$ : 2 bars,  $\text{pH}_2\text{S}$ : 0.13 bar, free HAC: 1,000 ppm,  $T_g$ : 70°C, WCR: 0.25 mL/m<sup>2</sup>/s,  $V_g$ : 5 m/s, exposure time: 3 weeks).

12. R. Nyborg, A. Dugstad, "Top-of-the-Line Corrosion and Water Condensation Rates in Wet Gas Pipelines," CORROSION/2007, paper no. 07555 (Houston, TX: NACE, 2007).
13. D. Hinkson, M. Singer, Z. Zhang, S. Nešić, "A Study of the Chemical Composition and Corrosivity of the Condensate in Top-of-the-Line Corrosion," CORROSION/2008, paper no. 08466 (Houston, TX: NACE, 2008).
14. A. Camacho, M. Singer, B. Brown, S. Nešić, "Top-of-the-Line Corrosion in H<sub>2</sub>S/CO<sub>2</sub> Environments," CORROSION/2008, paper no. 08470 (Houston, TX: NACE, 2008).
15. R. Nyborg, A. Dugstad, T. Martin, "Top-of-Line Corrosion with High CO<sub>2</sub> and Traces of H<sub>2</sub>S," CORROSION/2009, paper no. 09283 (Houston, TX: NACE, 2009).
16. J. Cai, D. Pugh, F. Ibrahim, S. Venaik, S. Asher, J. Pacheco, A. Dhokte, W. Sisak, E. Wright, D. Robson, "Top-of-Line Corrosion Mechanism for Sour Wet Gas Pipelines," in CORROSION/2009, paper no. 09285 (Houston, TX: NACE, 2009).
17. M. Bonis, "Form Sweet to Sour TLC: What's Different?" 2nd Int. TLC Conference (Bangkok: PTTEP, 2009).
18. A. Valdes, R. Case, M. Ramirez, A. Ruiz, "The Effect of Small Amounts of H<sub>2</sub>S on CO<sub>2</sub> Corrosion of Carbon Steel," CORROSION/1998, paper no. 22 (Houston, TX: NACE, 1998).
19. J. Kvaerkval, "The Influence of Small Amounts of H<sub>2</sub>S on CO<sub>2</sub> Corrosion of Iron and Carbon Steel," Eurocorr (Trondheim, Norway, 1997).
20. B. Brown, K.L. Lee, S. Nešić, "Corrosion in Multiphase Flow Containing Small Amounts of H<sub>2</sub>S," CORROSION/2003, paper no. 03341 (Houston, TX: NACE, 2003).
21. B. Brown, S. Reddy Parakala, S. Nešić, "CO<sub>2</sub> Corrosion in Presence of Trace Amounts of H<sub>2</sub>S," CORROSION/2004, paper no. 04736 (Houston, TX: NACE, 2004).
22. M. Singer, B. Brown, A. Camacho, S. Nešić, *Corrosion* 67, 1 (2011); p. 015004-1, doi:10.5006/1.3543715.
23. S. Smith, M. Joosten, "Corrosion of Carbon Steel by H<sub>2</sub>S in CO<sub>2</sub>-Containing Environments," CORROSION/2006, paper no. 06115 (Houston, TX: NACE, 2006).
24. B.F.M. Pots, S.D. Kapusta, R.C. John, M.J.J. Simon Thomas, I.J. Rippon, T.S. Whitham, M. Girgis, "Improvements on de-Waard Williams Corrosion Prediction and Applications to Corrosion Management," CORROSION/2002 paper no. 02235 (Houston, TX: NACE, 2002).
25. S. Smith, "Discussion of the History and Relevance of the CO<sub>2</sub>/H<sub>2</sub>S Ratio," CORROSION/2011, paper no. 11065 (Houston, TX, NACE, 2011).
26. ASTM G46-94(2005), "Standard Guide for Examination and Evaluation of Pitting Corrosion" (West Conshohocken, PA: ASTM International, 2005).
27. ASTM G1-03, "Standard Practice for Preparing, Cleaning, and Evaluating Corrosion Test Specimens" (West Conshohocken, PA: ASTM International, 2003).